

Open set label noise learning with robust sample selection and margin-guided module

Yuandi Zhao^a, Qianxi Xia^b, Yang Sun^b, Zhijie Wen^{b,*}, Liyan Ma^c and Shihui Ying^{d,e}

^aCollege of Air Traffic Management, Civil Aviation University of China, 300300, Tianjin, China

^bDepartment of Mathematics, College of Sciences, Shanghai University, 200444, Shanghai, China

^cSchool of Computer Engineering and Science, Shanghai University, 200444, Shanghai, China

^dShanghai Institute of Applied Mathematics and Mechanics, Shanghai University, 200072, Shanghai, China

^eShanghai Institute of Applied Mathematics and Mechanics, Shanghai University, 200072, Shanghai, China

ARTICLE INFO

Keywords:

Learning with noise label
open set label noise learning
robust sample selection
margin ranking function

ABSTRACT

In recent years, the remarkable success of deep neural networks (DNNs) in computer vision is largely due to large-scale, high-quality labeled datasets. Training directly on real-world datasets with label noise may result in overfitting. The traditional method is limited to deal with closed set label noise, where noisy training data has true class labels within the known label space. However, there are some real-world datasets containing open set label noise, which means that some samples belong to an unknown class outside the known label space. To address the open set label noise problem, we introduce a method based on Robust Sample Selection and Margin-Guided Module (RSS-MGM). Firstly, unlike the prior clean sample selection approach, which only select a limited number of clean samples, a robust sample selection module combines small loss selection or high-confidence sample selection to obtain more clean samples. Secondly, to efficiently distinguish open set label noise and closed set ones, margin functions are designed to filter open-set data and closed set data. Thirdly, different processing methods are selected for different types of samples in order to fully utilize the data's prior information and optimize the whole model. Furthermore, extensive experimental results with noisy labeled data from benchmark datasets and real-world datasets, such as CIFAR-100N-C, CIFAR80N-O, WebFG-469, and Food101N, indicate that our approach outperforms many state-of-the-art label noise learning methods. Especially, it can more accurately divide open set label noise samples and closed set ones.

1. Introduction

Deep neural networks (DNNs) (Krizhevsky et al., 2012; Ren et al., 2015; Redmon and Farhadi, 2017; Xie et al., 2020; Luo et al., 2019) have made significant advances in the domain of computer vision with large-scale and high-quality labeled datasets (e.g. ImageNet (Deng et al., 2009) and MSCOCO (Lin et al., 2014)). These datasets contain a large number of data, providing sufficient training samples for models, reducing overfitting to some extent and improving the models' generalization capabilities. On the one hand, large-scale, high-quality annotations necessitate manual annotation, which takes up a substantial amount of time and resources. (Li et al., 2020; Wang et al., 2022; Wu et al., 2020; Sehwan et al., 2019). On the other hand, we may easily collect low-quality image data from image search engines and other platforms (Sun et al., 2021; Yang et al., 2018; Yao et al., 2020; Tanaka et al., 2018; Yao et al., 2018; Zhang et al., 2019; Liu et al., 2021; Sun et al., 2021). Label noise is unavoidable (Li et al., 2017; Xiao et al., 2015; Sun et al., 2020; Yao et al., 2019). Recent research shows that training with noise-labeled data would definitely influence model performance, particularly for deep neural networks with significant learning and memory abilities (Nettleton et al., 2010; Zhang et al., 2021; Arpit et al., 2017). Therefore, learning with noisy label (LNL) is essential to preserve model reliability and flexibility in real-world applications.

In real-world datasets, noisy labels can be classified into two types: closed-set noise and open-set noise. (Wang et al., 2018). As shown in Fig. 1, we use a search engine to collect a web dataset containing images labeled using the CIFAR-10 dataset but with different images. This dataset can be separated into three categories: a clean set, a closed set, and an open set. For example, the sample labeled "cat", the white background box represents the clean set, includes

*Corresponding author

✉ dyzhao@cauc.edu.cn (Y. Zhao); 1746260680@qq.com (Q. Xia); yhgsy@shu.edu.cn (Y. Sun); wenzhijie@shu.edu.cn (Z. Wen); wenzhijie@shu.edu.cn (L. Ma); shyings@shu.edu.cn (S. Ying)

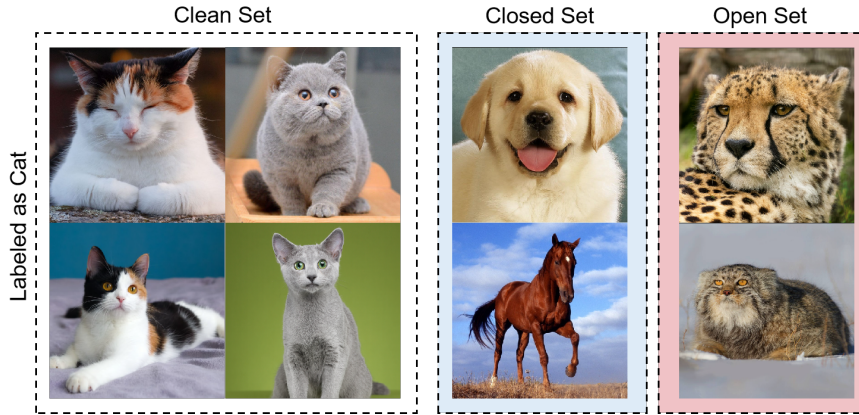


Figure 1: The example of open set label noise problem. Collecting a network dataset with labels from the CIFAR10 dataset but different images. Each image in the dataset is divided into three different groups: Clean Set, Closed Set, and Open Set. Clean Set refers to images with correct labels. Closed Set signifies images that are labeled incorrectly, yet their correct labels still exist within the known label space. Open Set indicates that the image is incorrectly labeled and the ground-truth label is outside the label space.

images that are actually cats. The blue background box represents the closed set, which includes images that are not cats but belong to other classes within the label space, such as dog or horse. And the red background box represents the open set, which includes images that are not cats and don't belong to any other classes within the label space, such as leopard or pallas cat. Closed set noise indicates that the true label of the noise sample is within the known label space of the training dataset \mathcal{Y}_{known} . In other words, the true class of the closed set noise sample falls within the category of classes which we are already familiar. In contrast, open set noise arises when the correct label for a noisy example lies outside the label space \mathcal{Y}_{known} defined by the training dataset, which means these samples belong to an unknown class not seen by the training set. In summary, closed-set noise samples are considered to be part of the data's in-distribution (ID), whereas open-set noise samples are part of the data's out-of-distribution (OOD).

In LNL, the majority of research primarily addresses the challenge of closed set label noise, such as loss correction (Lin et al., 2017; Ghosh et al., 2017; Zhang and Sabuncu, 2018), label correction (Wu et al., 2018; Reed et al., 2014; Arazo et al., 2019; Zheng et al., 2020), and sample selection (Zhang et al., 2017; Han et al., 2018; Lee et al., 2018). However, these solutions are frequently constrained when faced with practical application problems. Meanwhile, open set noisy labels often appear in real-world datasets and tend to present a more intricate challenge. Despite this, several studies already explore this issue, such as ILON (Wang et al., 2018), which selects clean samples using an iterative learning framework, has begun looking into the open-set noisy labels problem. In addition, InsCorr (Xia et al., 2021) uses partially discarded data information for semi-supervised learning. However, these methods frequently assume that the training dataset is only impacted by closed set noise or open set ones, without taking into account the possibility of both. EvidentialMix (Sachdeva et al., 2021) and MoPro (Li et al., 2020) propose that noise labels include both closed set noise or open set ones, but they don't use the information from the discarded data. Jo-SRC (Yao et al., 2021) and PNP (Sun et al., 2022) attempt to identify mislabeled open set data, whereas Co-mining (Cai et al., 2023) seeks to differentiate between hard samples and noisy samples by creating discriminative and robust feature spaces. However, due to the unavailability and diversity of open set samples, the model has difficulty identifying them. In some cases, the model is unable to successfully distinguish open set samples from clean data.

In this paper, we propose a novel deep learning method called Robust Sample Selection and Margin-Guided Module (RSS-MGM), which aims to address the challenges posed by closed-set noise and open-set noise on image classification tasks. To address these issues, we focus on sample selection methods that enhance the robustness and reliability of the model by combining robust sample selection and margin-guide learning.

First the robust sample selection module combines a small loss selection or high confidence sample selection, which can select more clean samples. The Jensen-Shannon (JS) divergence is selected to measure the similarity between predicted probabilities and true labels to identify clean samples. Then, we calculate the confidence scores of the samples to further filter the clean samples and construct a bigger clean sample subset. Second, we introduce the margin-guided module, which distinguishes between ID and OOD samples. We propose margin functions to choose open set samples

and closed set ones based on their respective properties. Then, the training dataset is divided into three sets: clean set, closed set, and open set. Finally, to address different types of samples, we employ a customized loss function. For clean samples, we use a cross-entropy loss function. For ID noise samples, we use a specific loss function and introduce a consistency regularization loss to improve the consistency and generalization ability of the model.

The main contributions of this paper are summarized as follows:

1. We propose a RSS-MGM method, a novel algorithmic framework for learning with open-set noisy labels. The framework makes use of the model's prediction and the unique characteristics of OOD samples to correct ID samples and filter out OOD samples.

2. Compared with traditional small-loss selection methods, our framework includes a high-confidence sample selection method that significantly improves the model's recognition performance for clean samples. This strategy is innovative in that it not only increases the model's capacity to recognize open-set samples in noisy data sets, but it also optimizes the model's overall learning process, ensuring the effective utilization of high-quality samples.

3. Considering the complexity and diversity of OOD samples, we design a margin-guided module. This module employs margin functions that can accurately identify and separate OOD samples and ID samples. This improves the model's capacity to handle outliers and edge cases.

4. Experiments conducted on the standard and real-world datasets CIFAR-100N-C, CIFAR80N-O, WebFG-496, and Food101N indicate that our method outperforms other advanced algorithms, particularly in OLN. Furthermore, experiments are used to verify the validity and reasonableness of the algorithm components.

The remainder of the paper is structured as follows. In Section 2, we provide an overview of the background on learning with open-set label noise. In Section 3, we describe the RSS-MGM method in detail. Experimental results are shown in Section 4. Finally, the paper is summarized in Section 5.

2. Related Works

Learning With Noisy Label Several methods have been proposed for LNL, such as loss correction (Lin et al., 2017; Ghosh et al., 2017; Zhang and Sabuncu, 2018), label correction (Wang et al., 2022; Wu et al., 2018; Reed et al., 2014; Arazo et al., 2019; Zheng et al., 2020; Albert et al., 2023; Xu et al., 2023), and sample selection (Zhang et al., 2017; Han et al., 2018; Lee et al., 2018; Yu et al., 2019; Pleiss et al., 2020; Cheng et al., 2020; Zhu et al., 2021; Zhang et al., 2022; Cordeiro et al., 2023; Wen et al., 2023; Li et al., 2024).

Loss Correction aims to adjust the loss function to mitigate the influence of noise labels while training. For instance, Lin et al. (Lin et al., 2017) develop the Focal Loss, which use an adjustable parameter to reduce the influence of noise labels on easily classified samples. Ghosh et al. (Ghosh et al., 2017) propose the Mean Absolute Error (MAE) Loss, which use absolute error in evaluating the difference between predicted labels and true labels. Conversely, the Cross-Entropy (CE) Loss emphasizes challenging samples and reduces the influence of noisy samples by modifying the weights of the loss function. In addition, Zhang et al. (Zhang and Sabuncu, 2018) generalize CE Loss to GCE Loss, which includes an adjustable parameter to alter the weighting for different classes, increasing the model's robustness to noisy samples.

Label correction aims to improve the quality of training data by estimating and correcting noisy labels. Wu et al. (Wu et al., 2018) propose using a similar neighborhood of clean data to train a classifier and assign pseudo-labels to noisy samples. Reed et al. (Reed et al., 2014) propose the Bootstrapping technique to handle noisy labels. Arazo et al. (Arazo et al., 2019) propose an unsupervised label noise modeling and loss correction, which automatically learns the probability distribution of noisy labels and adjusts the loss function. Zheng et al. (Zheng et al., 2020) propose an error-constrained label correction method to limit the range of label correction.

Sample selection efficiently filter training samples in order to reduce the interference of noisy labels. Zhang et al. (Zhang et al., 2017) propose a sample mixing strategy (Mixup) that linearly estimates features from several samples, generating new samples for training. Han et al. (Han et al., 2018) propose Co-teaching, where two models collaborate by selecting samples to train each other. Lee et al. (Lee et al., 2018) propose CleanNet, which uses feature vector similarity to choose clean samples through pruning. Li et al. (Li et al., 2024) proposed the Twin Binary Classification-Mixed Input (TBC-MI) method, which uses a twin binary classification network to transform complex multiclass classification problems into simpler binary classification tasks.

Open Set Label Noise Learning Open set label noise learning (OLNL) attempts to developing more robust and reliable deep learning models by learning from real-world datasets that contain both open set noise and closed set one.

A variety of related works have been proposed. For instance, Wang et al. (Wang et al., 2018) design an iterative learning framework that enables effective robust training on datasets with open set label noise. Sachdeva et al. (Sachdeva et al., 2021) specifically design the EvidentialMix framework to capture and analyze the impact of both open set and closed set noise. Xia et al. (Xia et al., 2021) employ instance correction techniques to adjust and optimize the instances of discarded data. Li et al. (Li et al., 2020) introduce Momentum Prototypes (MoPro), which effectively corrects ID samples and drops OOD samples. Yao et al. (Yao et al., 2021) propose a consistency-based method to identify open set noise. Sun et al. (Sun et al., 2022) achieve more accurate sample selection by modeling the consistency of different predictions for the same input sample. Cai et al. (Cai et al., 2023) focus on constructing a feature space to effectively distinguish between hard samples and noisy samples. Wan et al. (Wan et al., 2024) proposed Class Expansion Contrastive Learning (CECL), an innovative two-step contrastive learning framework designed to effectively handle open set label noise.

Contrastive Learning Contrastive learning (Chen et al., 2020a,b; Ortego et al., 2021) has grown in popularity in recent years due to its capacity to get key information from unlabeled data. This approach is making significant progress in a number of applications (Yang et al., 2021; Li et al., 2021). Specifically, each input image is randomly augmented, resulting in two augmented views of the image. Subsequently, the model is optimized using a contrastive loss function. This strategy enhances the model's capacity to differentiate image features, increasing the accuracy and robustness of the model. For instance, SimCLR (Chen et al., 2020a) is a simple yet effective contrastive learning framework that emphasizes the importance of data augmentation. MoCo (Chen et al., 2020b) establishes the concept of momentum contrast, which enhances stability by maintaining momentum updates in the network. PCL (Jiang et al., 2020) uses prototypes as cluster centers for contrastive learning in the primary subspace, which further enhancements utilizing weakly supervised contrastive losses and Mixup (Zhang et al., 2017). RRL (Li et al., 2021) aims to enhance model resilience to noisy data by adversarially addressing noise-induced interference. LaCoL (Yan et al., 2022) emphasizes the latent value of noise through negative correlation, aiming to mine information from noisy samples to enrich learning representations.

3. The Proposed Method: RSS-MGM

We define the training dataset as $\mathcal{D}(x_i, y_i)_{i=1}^N$, where x_i is an input image and $y_i = c \in \{1, \dots, C\}$ is its annotated label. Denote y_i^* as the ground-truth label of x_i .

Traditionally, it has been assumed that all annotated labels are correct (i.e., $y_i = y_i^*$), allowing the model to be optimized by minimizing experience loss.:

$$\mathcal{L} = \mathbb{E}_{\mathcal{D}}[l_{ce}(x_i, y_i)] = \frac{1}{N} l_{ce}(x_i, y_i), \quad (1)$$

in which,

$$l_{ce}(x_i, y_i) = - \sum_{c=1}^C y_i^c \log(p^c(x_i, \Theta)), \quad (2)$$

where Θ represents the model parameters, and $p^c(x_i, \Theta)$ represents the network's prediction that the sample x_i belongs to class c . For convenience, we represent $p^c(x_i, \Theta)$ as p_i^c . y_i^c indicates the class label for sample x_i in class c .

However, when a dataset contains noise labels (e.g., a web image dataset), the assumption that the labels are completely clean is incorrect. This is due to the difficulty of identifying the complexity of big and different datasets, which inevitably leads to labeling errors. Despite the high model capacity of DNNs, they often overfit to noisy labels because of the network's memorizing effect, severely impacting the model's classification accuracy and generalization ability (Zhang et al., 2017).

The aim of this research is to train the network on a dataset with label noise, including both open set noise and closed set one, with the goal of obtaining high accuracy on test set. By addressing the challenges given by these noisy labeled data, we hope to improve the network's robustness and classification performance in a wide range of real-world situations. Fig. 2 illustrates the algorithm's general logic and training framework. Specifically, the training dataset is augmented to generate a weakly augmented view and a strongly augmented view. These views are then fed into two separate networks with shared weights for prediction. The prediction results p^s and p^w , as well as the label y , are fed

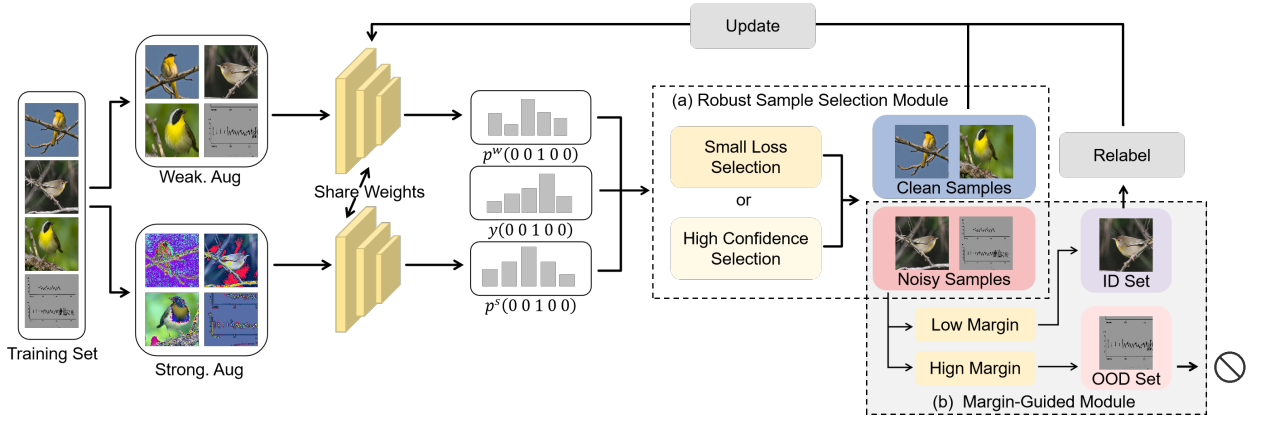


Figure 2: The overall framework of RSS-MGM. Each input image x_i is augmented into one weakly view and one strongly augmented view before being fed into the label predictor network, leading to two label predictions: p^w for the weakly augmented view and p^s for the strongly augmented view. Afterward, based on the Robust Sample Selection Module, samples are classified as Clean Set or Noisy Set. If the sample is clean, it will be fed into the label prediction network. Otherwise, based on the Margin-Guided Module, samples are divided into ID Set or OOD Set. Samples from the ID Set will be re-labeled to update the network, while samples from the OOD Set will be directly discarded. Finally, our model is updated by back-propagating.

into (a) the robust sample selection module, which divides the training set into the clean set and the noise set. Then, the noise set is fed into (b) the margin-guided module, which further divides the noise set into ID set and OOD set. Samples from the the clean set and the ID sets are used to update the network, while samples from the OOD set are discarded.

3.1. Robust Sample Selection Module

When noisy labels are presence in the dataset, there is a possibility that the model will learn their incorrect relationships, causing a performance drop. Previous studies typically employ small-loss sample selection methods to choose clean samples. However, this approach often results in a small number of clean samples. This limitation becomes particularly problematic in OLNL, where continuing to use this method may exacerbate the performance decline of the model. To address this issue, we propose a robust sample selection module that filters bigger clean samples for network training.

We use the loss function to select samples and divide the training dataset into clean samples and noisy ones. DNNs tend to prioritize learning clean samples initially and progressively adapting to the inclusion of noisy samples (Li et al., 2017; Zhang et al., 2021). We select clean samples based on Jensen-Shannon (JS) divergence. For a sample x_i , we utilize JS divergence to measure the dissimilarity between the predicted distribution $p_i = [p_i^1, p_i^2, \dots, p_i^C]$ and its corresponding label distribution $y_i = [y_i^1, y_i^2, \dots, y_i^C]$.

$$d_i = D_{JS}(p_i || y_i) = \frac{1}{2} D_{KL}(p_i || \frac{p_i + y_i}{2}) + \frac{1}{2} D_{KL}(y_i || \frac{p_i + y_i}{2}), \quad (3)$$

in which

$$D_{KL}(p_i || p_j) = \sum_{c=1}^C p_i^c \log \frac{p_i^c}{p_j^c}, \quad (4)$$

where $D_{KL}(p_i || p_j)$ is the Kullback-Leibler divergence, which measures the difference between two probability distributions.

A lower JS divergence indicates a higher similarity between the predicted distribution of the sample and its corresponding label distribution. Conversely, a higher JS divergence suggests a greater difference between them, potentially containing noise. Therefore, we can use JS divergence to select clean samples.

When considering the logarithm with base 2, the JS divergence is limited to 0 and 1. This can be regarded as a probability that the sample x_i is a clean sample.

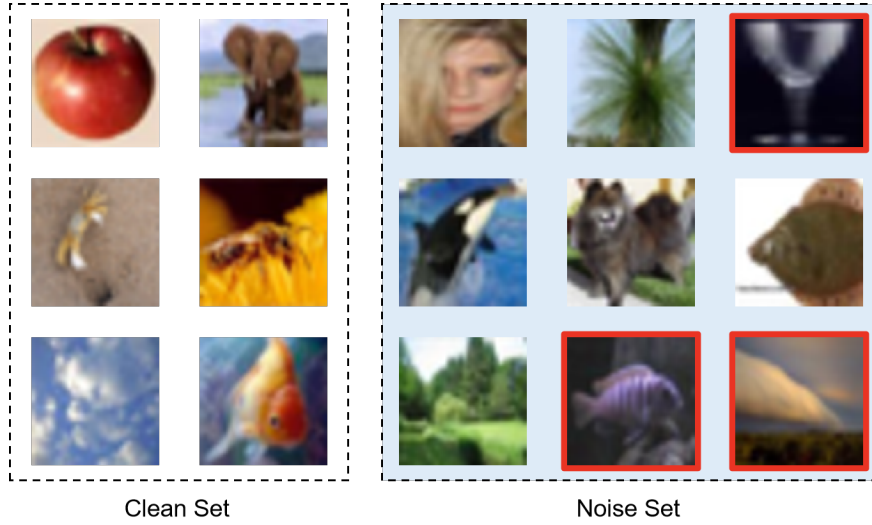


Figure 3: An example of the small loss selection method for dividing the training dataset. Here, Clean Set represents the set of samples that are identified as clean samples, which are considered to be labeled accurately. The Noise Set, on the other hand, represents the set of samples with noisy labels. However, the samples bordered in red in the noise set are actually clean, but are incorrectly classified in the noise set.

Then we define a \mathcal{P} as follows:

$$\mathcal{P} = 1 - d_i. \quad (5)$$

After introducing a threshold τ_s , we filter out samples with probabilities below this threshold, resulting in our defined "clean" set,

$$\mathcal{D}_{c_s} = \{x_i | \mathcal{P}_i > \tau_s\}. \quad (6)$$

where \mathcal{D}_{c_s} refers to the clean sample set after small-loss selection.

Then, the "unclean" set can be represented as $\mathcal{D}_n = \mathcal{D} \setminus \mathcal{D}_{c_s}$. However, this selection strategy does not filter out all clean samples, making it unsuitable for OLNL. As shown in Figure 3, Clean Set and Noise Set represent the sets obtained by small-loss selection, respectively. The samples bordered in red in the noise set are clean, but are incorrectly selected into the noise set.

Inspired by the pseudo-labeling method used for semi-supervised learning (Sohn et al., 2020; Zhao et al., 2022; Wang et al., 2020; Gu et al., 2016), we create a larger clean set, ensuring its quality. Specifically, we define the confidence score for any given sample x_i as:

$$s_i = \sum_{j=1}^C f_j(x_i) \mathbb{I}(j = y_i), \quad (7)$$

where $f_j(x_i)$ represents the predicted probability of sample x_i belonging to class j , and the indicator function $\mathbb{I}(j = y_i)$ returns 1 when j matches the true label y_i and 0 otherwise.

Then, the bigger clean set can be calculated as follows:

$$\mathcal{D}_{c_h} = \{x_i | s_i > \tau_h\}, \quad (8)$$

where \mathcal{D}_{c_h} refers to the clean sample set after high confidence sample selection, τ_h is a discriminative threshold to divide samples into two groups based on their confidence scores s_i : confident samples and unconfident ones.

Finally, we can combine \mathcal{D}_{c_s} and \mathcal{D}_{c_h} to obtain a complete clean dataset \mathcal{D}_c :

$$\mathcal{D}_c = \mathcal{D}_{c_s} \cup \mathcal{D}_{c_h}. \quad (9)$$

The noisy set \mathcal{D}_n is calculated as follows:

$$\mathcal{D}_n = \mathcal{D} \setminus \mathcal{D}_c. \quad (10)$$

3.2. Margin-Guided Module

In the previous section, we utilize the robust sample selection module to separate the training set \mathcal{D}_{train} into \mathcal{D}_c and \mathcal{D}_n . Despite the presence of label noise in the data from \mathcal{D}_n , it is vital to keep some samples and explore the possibility of re-labeling, particularly high confidence samples within the ID samples, as they can provide beneficial information for our model. (Zhang et al., 2022) Therefore, simply removing unclean samples is not a viable option. We need to distinguish the high confidence samples from the noisy samples and use them to improve the training of the model.

In DNNs, the model's predictions are usually limited by the known label space. As a result, when dealing with OOD samples, the model's predictions frequently display higher label uncertainty, resulting in a nearly uniform distribution of predicted probabilities, and predicted probabilities are closer to each other. In contrast, for ID samples, the predicted probability distribution resembles a one-hot distribution, with one probability reaching the highest value. In such cases, we can select samples based on the distribution of the predicted probabilities.

To fully utilize the information, we propose to divide \mathcal{D}_n into \mathcal{D}_{OOD} and \mathcal{D}_{ID} , where \mathcal{D}_{ID} requires further subdivision into \mathcal{D}_{high} and \mathcal{D}_{rest} . Next, we can discard OOD and rest samples directly, while for high confidence samples, we can use semi-supervised learning to make use of their information. To achieve this purpose, we present the Margin-Guided Module.

For OOD samples, the model's predictions have a greater label uncertainty, and the probability distribution is nearly uniform. As a result, the model's predictions barely different between two alternative augmentations of the same sample x_i . We develop a margin ranking function to filter OOD samples based on this property.

Specifically, We use two different augmentation approaches, weak augmentation $A^w(\cdot)$ and strong augmentation $A^s(\cdot)$, to create two alternative augmented views (e.g., $v^w = A^w(x_i)$ and $v^s = A^s(x_i)$) from a given sample x_i . Subsequently, these views are separately fed into the network to obtain prediction probabilities, p^w and p^s , respectively. Finally, we calculate the margin between these two views as:

$$M_v = \mathbb{I}[\operatorname{argmax}_c p^w \neq \operatorname{argmax}_c p^s]. \quad (11)$$

Based on M_v , we can obtain \mathcal{D}_{OOD} :

$$\mathcal{D}_{OOD} = \{x_i | M_v^i \cdot \mathcal{D}_n, x_i \in \mathcal{D}_n\}. \quad (12)$$

And the ID set can be obtained through:

$$\mathcal{D}_{ID} = \mathcal{D}_n \setminus \mathcal{D}_{OOD}. \quad (13)$$

Thus, we have divided \mathcal{D}_n into \mathcal{D}_{OOD} and \mathcal{D}_{ID} .

After that, we process \mathcal{D}_{ID} further. The differences in the predicted probabilities for sample x_i are remarkable since the network's predicted probability for ID samples has a maximum. We design a margin ranking function to eliminate high confidence samples in order to take advantage of these feature.

Specifically, for a given sample x_i , we calculate the difference between the largest value and second largest value of the model output. This measures the difference between the prediction class of the network and other classes. The margin function is defined as follows:

$$M = z_y(x_i) - \max_{k \neq y} z_k(x_i), \quad (14)$$

where $z_y(x_i)$ represents the logit of the network's prediction for sample x_i with class y , $\max_{k \neq y} z_k(x_i)$ is the maximum logit value of the network's prediction for sample x_i among all classes except class y . In other words, it is the highest logit value for all classes other than class y in the network's prediction for sample x_i .

The higher the margin value, the higher confidence of the model, enabling us to utilize the information from these samples for semi-supervised learning. On the contrary, lower margin values indicate lower confidence in the model's predictions, suggesting potential uncertainty. This uncertainty may lead to a decrease in the model's classification performance. Therefore, we are less likely to employ the information obtained from these samples.

To ensure fairness, we consider two different views of the same sample (e.g., v^w and v^s).

$$M_p = \frac{1}{2}(M_{p^w} + M_{p^s}), \quad (15)$$

where

$$M_{p^w} = z_y(v^w) - \max_{k \neq y} z_k(v^w), \quad (16)$$

$$M_{p^s} = z_y(v^s) - \max_{k \neq y} z_k(v^s). \quad (17)$$

Consequently, given τ_p , \mathcal{D}_{high} is defined as follows:

$$\mathcal{D}_{high} = \{x_i | M_p^i > \tau_p \text{ and } x_i \in \mathcal{D}_{ID}\}. \quad (18)$$

The remaining samples are indicated as \mathcal{D}_{rest} :

$$\mathcal{D}_{rest} = \mathcal{D}_{ID} \setminus \mathcal{D}_{high}. \quad (19)$$

This way, we successfully partition \mathcal{D}_n into \mathcal{D}_{OOD} and \mathcal{D}_{ID} , with \mathcal{D}_{ID} further divided into \mathcal{D}_{high} and \mathcal{D}_{rest} .

3.3. Label Reassignment

In the first two parts, we successfully divide the training dataset \mathcal{D} into \mathcal{D}_c , \mathcal{D}_{OOD} , and \mathcal{D}_{ID} . Next, we apply different processing strategies on these three subdatasets.

For \mathcal{D}_{clean} , we assume that all sample labels are correct, thus we keep the sample labels. To improve generalization performance, we use label smoothing regularization (LSR) (Yao et al., 2021) to calculate the loss of clean samples, which transform their labels $y_i^c \in \{1, \dots, C\}$ to \tilde{y}_i^c .

$$\tilde{y}_i^c = \begin{cases} 1 - \epsilon, & c = y_i^c \\ \frac{\epsilon}{C-1}, & c \neq y_i^c \end{cases}, \quad (20)$$

where ϵ is a hyperparameter that controls the smoothness of the label distribution.

For \mathcal{D}_{ID} , we believe that \mathcal{D}_{high} can provide valuable information, therefore, we adopt a re-labeling strategy. Specifically, we use temperature-based sharpening method to deal with these samples. We introduce a temperature parameter τ to modify the original network prediction probabilities p_i , which generates sharpened predictions \hat{p}_i .

$$\hat{p}_i = \frac{p_i^{\frac{1}{\tau}}}{\sum_j p_j^{\frac{1}{\tau}}}, \quad (21)$$

where p_i represents the original prediction of sample x_i , and τ is the temperature parameter used for sharpening.

Consider the model's consistency in predicting different augmented views of sample x_{id} within the same distribution. We obtain pseudo-labels for each sample by calculating the average probabilities of two different views. Therefore, the calculation of the same sample x_i forecast the probability of two different augmentation $p_{x_i}^w$ and $p_{x_i}^s$, and take its averaging \bar{p}_i ,

$$\bar{p}_i = \frac{1}{2}(p_{x_i}^w + p_{x_i}^s). \quad (22)$$

Specifically for \mathcal{D}_{rest} , we consider that \mathcal{D}_{rest} samples provide limited useful information and can be disregarded.

For \mathcal{D}_{ood} , we remove these samples from the training set. There are two primary reasons. First, OOD samples may introduce unexpected changes and perturbations, affecting the model's generalization ability. Second, the labels of OOD samples do not fall inside the known label space, which may provide additional uncertainty in the model's predictions of OOD data.

3.4. The Loss Function

When dealing with different subsets, we apply different loss functions for optimizing. For \mathcal{D}_c , we utilize the traditional cross entropy loss function, which is defined as follows:

$$\mathcal{L}_c = - \sum_{i \in \mathcal{D}_c} \left(\sum_{c=1}^C y_i^c \log p_i^c - \sum_{c=1}^C p_i^c \log(p_i^c) \right), \quad (23)$$

where C denotes the number of classes, y_i^c is the ground-truth label of sample x_i , p_i^c is the model's predicted probability for sample x_i belonging to class c , and $\mathbb{1}(\cdot)$ is the indicator function.

For \mathcal{D}_{high} , we propose an improved cross-entropy loss function as follows:

$$\mathcal{L}_n = - \sum_{i \in \mathcal{D}_{id}} \sum_{c=1}^C y_i^c \log \left(\frac{1}{2} p_i^w + \frac{1}{2} p_i^s \right) - \lambda \sum_{c=1}^C p_i^c \log(p_i^c), \quad (24)$$

where C denotes the number of classes, y_i^c is the ground-truth label of sample x_i , p_i^w represents the model's prediction for the weak augmented view x_i^w of the sample x_i , p_i^s represents the model's prediction for the strong augmented view x_i^s of the sample x_i , $\mathbb{1}(\cdot)$ is the indicator function and λ is the hyperparameter controlling the weight of the entropy regularization term.

We introduce a consistency regularization loss \mathcal{L}_{cons} to encourage well-trained models to maintain consistency when predicting different augmentations of the sample x_i .

$$\mathcal{L}_{cons} = \frac{1}{2} \sum_{i \in \mathcal{D}} [KL(p_i^w \parallel p_i^s) + KL(p_i^s \parallel p_i^w)], \quad (25)$$

where \mathcal{D} represents the training set, p_i^w and p_i^s is the predicted distributions for sample x_i from weak and strong augmented views, respectively. $KL(\cdot \parallel \cdot)$ represents the Kullback-Leibler (KL) divergence.

The overall loss function can be represented as:

$$\mathcal{L}_{total} = \mathcal{L}_c + \lambda_1 \mathcal{L}_n + \lambda_2 \mathcal{L}_{cons}, \quad (26)$$

where λ_1 and λ_2 are hyper-parameters.

4. Experiments

In this section, we report the results of the RSS-MGM method and compare it with some state-of-the-art algorithms. Specifically, we evaluate the effectiveness of the proposed method on four benchmark datasets: CIFAR100N-C, CIFAR80N-O (Krizhevsky et al., 2009), WebFG-496 (Sun et al., 2021), and Food101N (Bossard et al., 2014). Finally, ablation studies demonstrate the effectiveness of RSS-MGM.

4.1. Datasets and experimental settings

CIFAR100N-C and CIFAR80N-O CIFAR100N-C and CIFAR80N-O are synthetic noise datasets created based on the CIFAR100 dataset using predefined criterion (Krizhevsky et al., 2009). The original CIFAR100 dataset consists of 100 classes, with each containing 600 images of size 32×32 . There are 500 training images and 100 testing images per class. Each image comes with two labels: coarse-labels and fine-labels, corresponding to the classes and superclass. Both the training set and validation sets are affected by label noise. The predefined criterion for generating synthetic noise data sets are shown as follows:

CIFAR100N-C (Closed Set): This dataset builds on CIFAR-100 by adding label noise. A label transition matrix \mathcal{Q} is utilized, with $\mathcal{Q}_{ij} = Pr[\tilde{y} = j | y = i]$ denotes the likelihood of converting a clean label y into a noisy label \tilde{y} . The noise rate n_c varies between 0 and 1, and the noise type \mathcal{T} can be either symmetric or asymmetric.

CIFAR80N-O (Open Set): In this dataset, the last 20 classes of CIFAR-100 are considered as OOD classes. Random noise based on \mathcal{T} is then introduced to the labels of the remaining samples, with a noise ratio of n_c . This process results in an overall noise ratio of $n_{all} = 0.2 + 0.8n_c$.

Algorithm 1 RSS-MGS Algorithm

Require: Training set $\mathcal{D} = \{(x^{(n)}, y^{(n)})_{n=1}^N\}$, network f with parameters Θ , learning rate η , epoch T_{\max} , iterations I_{\max}

Ensure: Updated network f

- 1: **for** $t = 1$ to T_{\max} **do**
- 2: Shuffle training set \mathcal{D} ;
- 3: **for** $n = 1$ to I_{\max} **do**
- 4: Fetch mini-batch \mathbb{B} from \mathcal{D} ;
- 5: Calculate $p_i = f(x_i, \Theta)$ for a sample x_i ;
- 6: Calculate d_i and s_i by Eq. (3) and Eq. (7);
- 7: Select \mathbb{B}_{c_c} and \mathbb{B}_{c_h} of \mathbb{B} according to Eq. (6) and Eq. (8);
- 8: Obtain the clean set \mathbb{B}_c by Eq. (9) and the unclean set \mathbb{B}_n by Eq. (10);
- 9: **if** sample x_i in \mathbb{B}_c **then**
- 10: Label smoothing regularization to x_i by Eq. (20);
- 11: **else**
- 12: Generate two different views $v^w = A^w(x_i)$ and $v^s = A^s(x_i)$;
- 13: Calculate predicted probabilities p^w and p^s for v^w and v^s ;
- 14: Calculate margin function M_v and M_p by Eq. (11) and Eq. (15);
- 15: Obtain \mathbb{B}_{OOD} and \mathbb{B}_{ID} by Eq. (12) and Eq. (13);
- 16: Divide \mathbb{B}_{ID} into \mathbb{B}_{high} and \mathbb{B}_{rest} by Eq. (18) and Eq. (19);
- 17: **for** sample x_i in \mathbb{B}_{high} **do**
- 18: Sharpen predicted probabilities \hat{p}_i by Eq. (21);
- 19: Calculate pseudo-labels for x_i by Eq. (22);
- 20: **end for**
- 21: **end if**
- 22: Calculate loss \mathcal{L}_{total} by Eq. (26);
- 23: Update $\Theta = \Theta - \eta \nabla L$.
- 24: **end for**
- 25: **end for**

WebFG-496 WebFG-496 (Sun et al., 2021) is divided into three sub-datasets: Web-Airplan, Web-Bird, and Web-Car. It contains 53,339 web training images of 200 bird species (Web-bird), 100 aircraft types (Web-aircraft), and 196 car models (Web-car). Since the WebFG-496 dataset is obtained from the network, image labels may contain a certain level of noise. As a result, it is unnecessary to manually add label noise during the study.

Food101N Food101N (Bossard et al., 2014) is a large-scale image dataset, obtained from the Internet. This dataset consists 310,009 images of food recipes classified in 101 classes. It is essential to point out that because images are collected from accessible web resources the images are not clean, and thus still contain some amount of noise labels. So that, this dataset does not require any manual label noise injections.

Experimental settings Following Jo-SRC (Yao et al., 2021), we employ a 7-layer DNN network model for CIFAR100N-C and CIFAR80N-O. We use the Adam optimizer with a momentum of 0.9. The initial learning rate is set to 0.001, and the batch size is 128. The overall training consists of 300 epochs, with 10 epochs for pre-training and 290 for the main training phase. A linear decay of the learning rate to 10^{-4} commences after 80 epochs. In the process of filtering clean samples, the relevant parameters τ_s and τ_h are set to 0.75 and 0.9. During the margin ranking function sample selection phase, the relevant parameters τ_p is set to 0.9. The selection coefficients λ_1 and λ_2 are set to 0.05 eachare both set to 0.05. For Web-Aircraft, Web-Bird, and Web-Car, we employ a pre-trained ResNet-50 model trained on ImageNet as our backbone. Network parameters are updated using the SGD optimizer with a momentum of 0.9, and the initial learning rate is set to 0.0005. Due to the larger image size in the Web-Car dataset and hardware limitations, the batch size for this experiment is limited to 16. The total training duration comprises 200 epochs, with 10 epochs designated for pre-training and 190 epochs for the main training phase. Learning rate decay is implemented through a cosine annealing schedule, commencing after the warmup period. All other parameters are

maintained consistently with those used for the CIFAR datasets. For Food101N, we follow the settings outlined in Jo-SRC, utilizing a pre-trained ResNet-50 for comparison. Parameters remain consistent with those employed on the CIFAR datasets.

Baselines We compare RSS-MGM (Algorithm 1) with the following state-of-the-art algorithms. All methods are implemented in PyTorch with default parameters, and all experiments are conducted on an NVIDIA GeForce RTX 3090 GPU. To assess the performance of RSS-MGM on CIFAR100N-C and CIFAR80N-O, we compare RSS-MGM with the following state-of-the-art sample selection methods: Decoupling (Malach and Shalev-Shwartz, 2017), Co-teaching (Han et al., 2018), Co-teaching+ (Yu et al., 2019), JoCoR (Wei et al., 2020), Jo-SRC (Yao et al., 2021), and PNP (Sun et al., 2022). To evaluate the effectiveness of RSS-MGM on Web-Aircraft, Web-Bird, and Web-Car, in addition to the above methods, we also compare it with the following methods: SELFIE (Song et al., 2019), PENCIL (Yi and Wu, 2019), AFM (Peng et al., 2020), CRSSC (Sun et al., 2020), Self-adaptive (Huang et al., 2020), DivideMix (Li et al., 2020), PLC (Zhang et al., 2021), Peer-learning (Sun et al., 2021). For the evaluation on Food101N, we compare the following methods with ours: CleanNet (Lee et al., 2018), DeepSelf (Han et al., 2019), Jo-SRC (Yao et al., 2021) and PNP (Sun et al., 2022). Finally, direct training on noisy datasets serves as a straightforward baseline (referred to as Standard) for comparison.

4.2. The experiments on Synthetic Noisy Datasets

Results on CIFAR100N-C. Although our method is intended to simulate real-world (open-set) noise situations, it is equally effective in closed-set situations. Table 1 shows the test accuracies for CIFAR100N-C. The results of existing approaches are sourced from Jo-SRC (Wei et al., 2020), under same experimental settings as our approach.

Under symmetric noise conditions, our method achieves remarkable average test accuracies of 64.6%, 60.28%, and 41.88% at 20%, 50%, and 80% noise rates, respectively. This demonstrates the adaptability of RSS-MGM to varied levels of symmetric noise. RSS-MGM outperforms the prior PNP approach (54.92%) in a Symmetric-50% noise environment, achieving an average test accuracy of 60.28%. This outcome highlights the superiority of our method in dealing with common symmetric noise situations.

Even more remarkable is its performance in the presence of asymmetric noise. Our method achieves a high test accuracy of 64.06% at Asymmetric-20%. RSS-MGM performs well in the difficult Asymmetric-40% noise environment, with an average test accuracy of 58.36%. These findings demonstrate that RSS-MGM achieves strong performance not only under typical symmetric noise conditions but also in scenarios involving more challenging asymmetric noise. This robustness is critical for real-world applications that frequently confront complex and actual noise situations.

Results on CIFAR80N-O. CIFAR80N-O is specifically designed to simulate real-world (open-set) noise scenarios. In Table 2, we provide a comparison between our method and state-of-the-art approaches. Similarly, the results of existing methods are derived from Jo-SRC (Wei et al., 2020). Our methodology is assessed under identical experimental conditions.

Under Symmetric noise conditions, the method achieves average test accuracies of 67.32%, 61.59%, and 39.86% for noise rate of 20%, 50%, and 80%, respectively. These extraordinary results demonstrate our approach robustness in the face of varied degrees of symmetric noise, particularly in high-intensity noise environments where it maintains relatively high accuracy.

At 20% Asymmetric noise, the approach achieves an average test accuracy of 61.23%, significantly outperforming other methods and demonstrating its exceptional capabilities in mild non-symmetric noise conditions. Our method performs well in the complicated noise environment of Asymmetric-40%, with an average test accuracy of 59.80%. This result highlights the stability of RSS-MGM, which performs not only in symmetric noise but also in more challenging and real-world asymmetric noise issues.

4.3. The experiments on Real-world Noisy Datasets

In addition to the evaluations shown above, we conduct experiments on real-world noisy datasets, such as the Web-Aircraft/Bird/Car and Food01N datasets, to validate the effectiveness of RSS-MGM.

Results on Web-Aircraft / Bird / Car. Web-Aircraft, Web-Bird, and Web-Car are three real-world web image datasets designed for fine-grained visual classification applications. These datasets differ from others in that over 25% of the samples have unknown asymmetric noise labels, and no label validation information is provided. This

Table 1

Average test accuracy (%) on CIFAR100N-C over the last 10 epochs ("Sym" and "Asym" denote the symmetric and asymmetric label noise, respectively).

Methods	Syms-20%	Syms-50%	Syms-80%	Asym-20%	Asym-40%
Standard	35.14 ± 0.44	16.97 ± 0.40	4.41 ± 0.14	34.74 ± 0.53	27.29 ± 0.25
Decoupling(Malach and Shalev-Shwartz, 2017)	33.10 ± 0.12	15.25 ± 0.20	3.89 ± 0.16	33.89 ± 0.23	26.11 ± 0.39
Co-teaching(Han et al., 2018)	43.73 ± 0.16	34.96 ± 0.50	15.15 ± 0.46	35.82 ± 0.38	28.35 ± 0.25
Co-teaching+(Yu et al., 2019)	49.27 ± 0.03	40.04 ± 0.70	13.44 ± 0.37	40.03 ± 0.64	33.62 ± 0.39
JoCoR(Wei et al., 2020)	53.01 ± 0.04	43.49 ± 0.46	15.49 ± 0.98	39.78 ± 0.38	32.70 ± 0.35
Jo-SRC(Yao et al., 2021)	58.15 ± 0.14	51.26 ± 0.11	23.80 ± 0.05	63.96 ± 0.10	38.52 ± 0.20
PNP(Sun et al., 2022)	64.25 ± 0.12	53.74 ± 0.21	31.32 ± 0.19	63.65 ± 0.12	60.25 ± 0.21
RSS-MGM	64.60 ± 0.08	60.28 ± 0.09	41.88 ± 0.12	64.06 ± 0.15	58.36 ± 0.13

Table 2

Average test accuracy (%) on CIFAR80N-O over the last 10 epochs ("Sym" and "Asym" denote the symmetric and asymmetric label noise, respectively).

Methods	Syms-20%	Syms-50%	Syms-80%	Asym-20%	Asym-40%
Standard	29.37 ± 0.09	13.87 ± 0.08	4.20 ± 0.07	28.97 ± 0.04	22.25 ± 0.08
Decoupling(Malach and Shalev-Shwartz, 2017)	43.49 ± 0.39	28.22 ± 0.19	10.01 ± 0.29	-	33.74 ± 0.26
Co-teaching(Han et al., 2018)	60.38 ± 0.22	52.42 ± 0.51	16.59 ± 0.27	-	42.42 ± 0.30
Co-teaching+(Yu et al., 2019)	53.97 ± 0.26	46.75 ± 0.14	12.29 ± 0.09	-	43.01 ± 0.59
JoCoR(Wei et al., 2020)	59.99 ± 0.13	50.61 ± 0.12	12.85 ± 0.05	43.56 ± 0.25	39.37 ± 0.16
Jo-SRC(Yao et al., 2021)	65.83 ± 0.13	58.51 ± 0.08	29.76 ± 0.09	66.96 ± 0.06	53.03 ± 0.25
PNP(Sun et al., 2022)	67.00 ± 0.18	54.92 ± 0.10	34.36 ± 0.18	65.51 ± 0.10	61.23 ± 0.17
RSS-MGM	67.32 ± 0.15	61.59 ± 0.13	39.86 ± 0.08	67.02 ± 0.08	59.80 ± 0.16

Table 3

Comparison with state-of-the-art approaches in test accuracy (%) on Web-Aircraft, Web-Bird, and Web-Car.

Methods	Web-Aircraft	Web-Bird	Web-Car
Standard	60.80	64.40	60.60
Decoupling(Malach and Shalev-Shwartz, 2017)	75.91	71.61	79.41
Co-teaching(Han et al., 2018)	79.54	76.68	84.95
Co-teaching+(Yu et al., 2019)	74.80	70.12	76.77
SELFIE(Song et al., 2019)	79.27	77.20	82.90
PENCIL(Yi and Wu, 2019)	78.82	75.09	81.68
JoCoR(Wei et al., 2020)	80.11	79.19	85.10
AFM(Peng et al., 2020)	81.04	76.35	83.48
CRSSC(Sun et al., 2020)	82.51	81.31	87.68
Self-adaptive(Huang et al., 2020)	77.92	78.49	78.19
DivideMix(Li et al., 2020)	82.48	74.40	84.27
Jo-SRC(Yao et al., 2021)	82.73	81.22	88.13
PLC(Zhang et al., 2021)	79.24	76.22	81.87
Peer-learning(Sun et al., 2021)	78.64	75.37	82.48
PNP(Sun et al., 2022)	85.54	81.93	90.11
RSS-MGM	85.82	82.34	90.15

feature makes these datasets more representative of real-world applications and provides an excellent experimental framework for investigating open-set noise label challenges. We validate our method using the same conditions as Jo-SRC's experimental methodology (Wei et al., 2020). Table 3 shows an overview of test accuracies for Web-Aircraft, Web-Bird, and Web-Car with current methods.

Results on Food101N. As shown in Table 4, the results of the study on the Food101N dataset show that RSS-MGM achieves higher test accuracy compared to existing state-of-the-art methods. These datasets have more complex label

Table 4

Comparison with state-of-the-art approaches in test accuracy (%) on Food101N.

Method	Test accuracy
Standard	84.51
CleanNet(Lee et al., 2018)	83.47
DeepSelf(Han et al., 2019)	85.11
Jo-SRC(Yao et al., 2021)	86.66
PNP(Sun et al., 2022)	87.50
RSS-MGM	88.73

Table 5

Ablation study with sym 20 (%) on CIFAR80N.

Method	Test accuracy(%)
RSS-MGM	67.32
RSS-MGM w/o RSSM & MGM	62.47
RSS-MGM w/o RSS	65.53
RSS-MGM w/o MGS	65.35
RSS-MGM w/o SSL	66.49

Table 6

Ablation study with sym 20 (%) on CIFAR80N.

Method	Test accuracy(%)
RSS-MGM	67.32
RSS-MGM w/o \mathcal{M}_v	64.75
RSS-MGM w/o \mathcal{M}_p	65.38

noise patterns than synthetic datasets, although at lower noise ratios. This complexity is a greater challenge. The results suggest that RSS-MGM can effectively reduce label noise in large-scale real-world applications, particularly in more complex and challenging settings.

4.4. Ablation study

To verify the effectiveness of every RSS-MGM module, we perform a set of ablation studies on the CIFAR80N-O dataset with a 20% symmetric noise rate. Firstly, the Robust Sample Selection module (RSS) and the Margin-Guided Module (MGM) are removed respectively, and then the two modules are removed at the same time. In addition, we conduct ablation study on Semi-Supervised Learning (SSL).

In its current condition, the RSS-MGM method achieves excellent results, with a test accuracy of 67.32%. However, when the RSS is removed, the model's performance dropped slightly to 65.53%. This indicates that RSS strongly selects clean samples, so decreasing interference of noisy data and improving model performance. Similarly, removing the MGM reduced test accuracy to 65.35%, showing the importance of MGM in learning margin information and distinguishing between open set and closed set noise samples. Further study shows that when RSS and MGM were removed at the same time, the model performance dropped to 62.47%. This indicates the complementarity of the two modules in their combined role, which work together to increase the model's robustness and performance. Finally, to show the effect of semi-supervised learning, removing the SSL module resulted in a test accuracy of 66.49%, which is 0.83% lower than in the full situation. It emphasizes the positive influence of SSL in enhancing model performance while re-labeling the closed-set data and removing open-set data. Table 5 shows the experimental results.

We design a set of ablation studies to show the necessity of two margin functions in the Margin-Guided Strategy Module. In these tests, we remove \mathcal{M}_v and \mathcal{M}_p , respectively, to get insight into their impact to the performance of RSS-MGM. Table 6 displays the results of our ablation studies conducted on the CIFAR80N-O dataset with a 20% symmetric noise rate.

5. Conclusion

In this research, we focus on tackling the difficulties of learning from real-world datasets that include both closed-set and open-set label noise. To deal with this problem, RSS-MGM is proposed in this paper, which employs a multi-level sample selection method to divide the training dataset that goes beyond simply deleting noisy labels. Instead, it reduces the interference from noisy labels while keeping data features. This method is developed with the complexity of real-world datasets, which is critical in practical applications. In the experimental section, we compare the performance of RSS-MGM on synthetic and real-world datasets, which outperforms many state-of-the-art methods. In conclusion, the RSS-MGM method provides satisfactory results when dealing with the open set noise label problem.

6. Conflict of Interest

The authors declare that they have no conflict of interest.

Acknowledgments

This research is supported by the National Key R & D Program of China(No. 2021YFA1003004),the Open Fund for Key Laboratory of Internet of Aircrafts (No. MHFLW202305), the Tianjin Education Commission Research Program Project (2023KJ239) and the Large-scale Numerical Simulation Computing Sharing Platform of Shanghai University.

Data Availability

The CIFAR-100 dataset is available at <https://www.cs.toronto.edu/~kriz/cifar.html>. The WebFG-469 dataset is available at <https://github.com/NUST-Machine-Intelligence-Laboratory/weblyFG-dataset>. The Food101N dataset is available at <https://kuanghuei.github.io/Food-101N/>.

References

- A. Krizhevsky, I. Sutskever, G. Hinton, Imagenet classification with deep convolutional neural networks, *Advances in neural information processing systems* 25 (2012).
- S. Ren, K. He, R. Girshick, J. Sun, Faster r-cnn: Towards real-time object detection with region proposal networks, *Advances in neural information processing systems* 28 (2015).
- J. Redmon, A. Farhadi, Yolo9000: better, faster, stronger, in: *Proceedings of the IEEE conference on computer vision and pattern recognition*, 2017, pp. 7263–7271.
- G.-S. Xie, L. Liu, F. Zhu, F. Zhao, Z. Zhang, Y. Yao, J. Qin, L. Shao, Region graph embedding network for zero-shot learning, in: *Computer Vision–ECCV 2020: 16th European Conference, Glasgow, UK, August 23–28, 2020, Proceedings, Part IV 16*, Springer, 2020, pp. 562–580.
- H. Luo, G. Lin, Z. Liu, F. Liu, Z. Tang, Y. Yao, Segeqa: Video segmentation based visual attention for embodied question answering, in: *2019 IEEE/CVF International Conference on Computer Vision (ICCV)*, IEEE, 2019, pp. 9666–9675.
- J. Deng, W. Dong, R. Socher, L.-J. Li, K. Li, L. Fei-Fei, Imagenet: A large-scale hierarchical image database, in: *2009 IEEE conference on computer vision and pattern recognition*, Ieee, 2009, pp. 248–255.
- T.-Y. Lin, M. Maire, S. Belongie, J. Hays, P. Perona, D. Ramanan, P. Dollár, C. L. Zitnick, Microsoft coco: Common objects in context, in: *Computer Vision–ECCV 2014: 13th European Conference, Zurich, Switzerland, September 6-12, 2014, Proceedings, Part V 13*, Springer, 2014, pp. 740–755.
- J. Li, R. Socher, S. C. Hoi, Dividemix: Learning with noisy labels as semi-supervised learning, *arXiv preprint arXiv:2002.07394* (2020).
- H. Wang, R. Xiao, Y. Dong, L. Feng, J. Zhao, Promix: combating label noise via maximizing clean sample utility, *arXiv preprint arXiv:2207.10276* (2022).
- S. Wu, X. Xia, T. Liu, B. Han, M. Gong, N. Wang, H. Liu, G. Niu, Class2simi: A new perspective on learning with label noise (2020).
- V. Schwag, A. N. Bhagoji, L. Song, C. Sitawarin, D. Cullina, M. Chiang, P. Mittal, Analyzing the robustness of open-world machine learning, in: *Proceedings of the 12th ACM Workshop on Artificial Intelligence and Security*, 2019, pp. 105–116.
- Z. Sun, Y. Yao, X.-S. Wei, Y. Zhang, F. Shen, J. Wu, J. Zhang, H. T. Shen, Webly supervised fine-grained recognition: Benchmark datasets and an approach, in: *Proceedings of the IEEE/CVF international conference on computer vision*, 2021, pp. 10602–10611.
- J. Yang, X. Sun, Y.-K. Lai, L. Zheng, M.-M. Cheng, Recognition from web data: A progressive filtering approach, *IEEE Transactions on Image Processing* 27 (2018) 5303–5315.
- Y. Yao, X. Hua, G. Gao, Z. Sun, Z. Li, J. Zhang, Bridging the web data and fine-grained visual recognition via alleviating label noise and domain mismatch, in: *Proceedings of the 28th ACM International Conference on Multimedia*, 2020, pp. 1735–1744.
- D. Tanaka, D. Ikami, T. Yamasaki, K. Aizawa, Joint optimization framework for learning with noisy labels, in: *Proceedings of the IEEE conference on computer vision and pattern recognition*, 2018, pp. 5552–5560.
- Y. Yao, F. Shen, J. Zhang, L. Liu, Z. Tang, L. Shao, Extracting multiple visual senses for web learning, *IEEE Transactions on Multimedia* 21 (2018) 184–196.

- W. Zhang, Y. Wang, Y. Qiao, Metacleaner: Learning to hallucinate clean representations for noisy-labeled visual recognition, in: Proceedings of the IEEE/CVF Conference on Computer Vision and Pattern Recognition, 2019, pp. 7373–7382.
- H. Liu, C. Zhang, Y. Yao, X.-S. Wei, F. Shen, Z. Tang, J. Zhang, Exploiting web images for fine-grained visual recognition by eliminating open-set noise and utilizing hard examples, *IEEE Transactions on Multimedia* 24 (2021) 546–557.
- Z. Sun, H. Liu, Q. Wang, T. Zhou, Q. Wu, Z. Tang, Co-Idl: A co-training-based label distribution learning method for tackling label noise, *IEEE Transactions on Multimedia* 24 (2021) 1093–1104.
- W. Li, L. Wang, W. Li, E. Agustsson, L. Van Gool, Webvision database: Visual learning and understanding from web data, *arXiv preprint arXiv:1708.02862* (2017).
- T. Xiao, T. Xia, Y. Yang, C. Huang, X. Wang, Learning from massive noisy labeled data for image classification, in: Proceedings of the IEEE conference on computer vision and pattern recognition, 2015, pp. 2691–2699.
- Z. Sun, X.-S. Hua, Y. Yao, X.-S. Wei, G. Hu, J. Zhang, Crssc: salvage reusable samples from noisy data for robust learning, in: Proceedings of the 28th ACM International Conference on Multimedia, 2020, pp. 92–101.
- Y. Yao, J. Zhang, F. Shen, L. Liu, F. Zhu, D. Zhang, H. T. Shen, Towards automatic construction of diverse, high-quality image datasets, *IEEE Transactions on Knowledge and Data Engineering* 32 (2019) 1199–1211.
- D. F. Nettleton, A. Orriols-Puig, A. Fornells, A study of the effect of different types of noise on the precision of supervised learning techniques, *Artificial intelligence review* 33 (2010) 275–306.
- C. Zhang, S. Bengio, M. Hardt, B. Recht, O. Vinyals, Understanding deep learning (still) requires rethinking generalization, *Communications of the ACM* 64 (2021) 107–115.
- D. Arpit, S. Jastrzyski, N. Ballas, D. Krueger, E. Bengio, M. S. Kanwal, T. Maharaj, A. Fischer, A. Courville, Y. Bengio, et al., A closer look at memorization in deep networks, in: International conference on machine learning, PMLR, 2017, pp. 233–242.
- Y. Wang, W. Liu, X. Ma, J. Bailey, H. Zha, L. Song, S.-T. Xia, Iterative learning with open-set noisy labels, in: Proceedings of the IEEE conference on computer vision and pattern recognition, 2018, pp. 8688–8696.
- T.-Y. Lin, P. Goyal, R. Girshick, K. He, P. Dollár, Focal loss for dense object detection, in: Proceedings of the IEEE international conference on computer vision, 2017, pp. 2980–2988.
- A. Ghosh, H. Kumar, P. S. Sastry, Robust loss functions under label noise for deep neural networks, in: Proceedings of the AAAI conference on artificial intelligence, volume 31, 2017.
- Z. Zhang, M. Sabuncu, Generalized cross entropy loss for training deep neural networks with noisy labels, *Advances in neural information processing systems* 31 (2018).
- X. Wu, R. He, Z. Sun, T. Tan, A light cnn for deep face representation with noisy labels, *IEEE Transactions on Information Forensics and Security* 13 (2018) 2884–2896.
- S. Reed, H. Lee, D. Anguelov, C. Szegedy, D. Erhan, A. Rabinovich, Training deep neural networks on noisy labels with bootstrapping, *arXiv preprint arXiv:1412.6596* (2014).
- E. Arazo, D. Ortego, P. Albert, N. O’Connor, K. McGuinness, Unsupervised label noise modeling and loss correction, in: International conference on machine learning, PMLR, 2019, pp. 312–321.
- S. Zheng, P. Wu, A. Goswami, M. Goswami, D. Metaxas, C. Chen, Error-bounded correction of noisy labels, in: International Conference on Machine Learning, PMLR, 2020, pp. 11447–11457.
- H. Zhang, M. Cisse, Y. N. Dauphin, D. Lopez-Paz, mixup: Beyond empirical risk minimization, *arXiv preprint arXiv:1710.09412* (2017).
- B. Han, Q. Yao, X. Yu, G. Niu, M. Xu, W. Hu, I. Tsang, M. Sugiyama, Co-teaching: Robust training of deep neural networks with extremely noisy labels, *Advances in neural information processing systems* 31 (2018).
- K.-H. Lee, X. He, L. Zhang, L. Yang, Cleannet: Transfer learning for scalable image classifier training with label noise, in: Proceedings of the IEEE conference on computer vision and pattern recognition, 2018, pp. 5447–5456.
- X. Xia, T. Liu, B. Han, M. Gong, J. Yu, G. Niu, M. Sugiyama, Instance correction for learning with open-set noisy labels, *arXiv preprint arXiv:2106.00455* (2021).
- R. Sachdeva, F. R. Cordeiro, V. Belagiannis, I. Reid, G. Carneiro, Evidentialmix: Learning with combined open-set and closed-set noisy labels, in: Proceedings of the IEEE/CVF Winter Conference on Applications of Computer Vision, 2021, pp. 3607–3615.
- J. Li, C. Xiong, S. C. Hoi, Mopro: Webly supervised learning with momentum prototypes, *arXiv preprint arXiv:2009.07995* (2020).
- Y. Yao, Z. Sun, C. Zhang, F. Shen, Q. Wu, J. Zhang, Z. Tang, Jo-src: A contrastive approach for combating noisy labels, in: Proceedings of the IEEE/CVF conference on computer vision and pattern recognition, 2021, pp. 5192–5201.
- Z. Sun, F. Shen, D. Huang, Q. Wang, X. Shu, Y. Yao, J. Tang, Pnp: Robust learning from noisy labels by probabilistic noise prediction, in: Proceedings of the IEEE/CVF Conference on Computer Vision and Pattern Recognition, 2022, pp. 5311–5320.
- Z. Cai, H. Liu, D. Huang, Y. Yao, Z. Tang, Co-mining: Mining informative samples with noisy labels, *Signal Processing* 209 (2023) 109003.
- P. Albert, E. Arazo, T. Krishna, N. E. O’Connor, K. McGuinness, Is your noise correction noisy? pls: Robustness to label noise with two stage detection, in: Proceedings of the IEEE/CVF Winter Conference on Applications of Computer Vision, 2023, pp. 118–127.
- C. Xu, R. Lin, J. Cai, S. Wang, Label correction using contrastive prototypical classifier for noisy label learning, *Information Sciences* 649 (2023) 119647.
- X. Yu, B. Han, J. Yao, G. Niu, I. Tsang, M. Sugiyama, How does disagreement help generalization against label corruption?, in: International Conference on Machine Learning, PMLR, 2019, pp. 7164–7173.
- G. Pleiss, T. Zhang, E. Elenberg, K. Q. Weinberger, Identifying mislabeled data using the area under the margin ranking, *Advances in Neural Information Processing Systems* 33 (2020) 17044–17056.
- H. Cheng, Z. Zhu, X. Li, Y. Gong, X. Sun, Y. Liu, Learning with instance-dependent label noise: A sample sieve approach, *arXiv preprint arXiv:2010.02347* (2020).
- C. Zhu, W. Chen, T. Peng, Y. Wang, M. Jin, Hard sample aware noise robust learning for histopathology image classification, *IEEE transactions on medical imaging* 41 (2021) 881–894.

- Y. Zhang, W. Deng, X. Cui, Y. Yin, H. Shi, D. Wen, Model and data agreement for learning with noisy labels, arXiv preprint arXiv:2212.01054 (2022).
- F. R. Cordeiro, R. Sachdeva, V. Belagiannis, I. Reid, G. Carneiro, Longremix: Robust learning with high confidence samples in a noisy label environment, *Pattern Recognition* 133 (2023) 109013.
- Z. Wen, H. Xu, S. Ying, Jsmix: a holistic algorithm for learning with label noise, *Neural Computing and Applications* 35 (2023) 1519–1533.
- Y. Li, Z. Guo, L. Wang, L. Xu, Tbc-mi : Suppressing noise labels by maximizing cleaning samples for robust image classification, *Information Processing & Management* 61 (2024) 103801. URL: <https://www.sciencedirect.com/science/article/pii/S0306457324001602>. doi:<https://doi.org/10.1016/j.ipm.2024.103801>.
- W. Wan, X. Wang, M.-K. Xie, S.-Y. Li, S.-J. Huang, S. Chen, Unlocking the power of open set: A new perspective for open-set noisy label learning, in: *Proceedings of the AAAI conference on artificial intelligence*, volume 38, 2024, pp. 15438–15446.
- T. Chen, S. Kornblith, M. Norouzi, G. Hinton, A simple framework for contrastive learning of visual representations, in: *International conference on machine learning*, PMLR, 2020a, pp. 1597–1607.
- X. Chen, H. Fan, R. Girshick, K. He, Improved baselines with momentum contrastive learning, arXiv preprint arXiv:2003.04297 (2020b).
- D. Ortego, E. Arazo, P. Albert, N. E. O’Connor, K. McGuinness, Multi-objective interpolation training for robustness to label noise, in: *Proceedings of the IEEE/CVF Conference on Computer Vision and Pattern Recognition*, 2021, pp. 6606–6615.
- J. Yang, Y. Bisk, J. Gao, Taco: Token-aware cascade contrastive learning for video-text alignment, in: *Proceedings of the IEEE/CVF International Conference on Computer Vision*, 2021, pp. 11562–11572.
- J. Li, C. Xiong, S. C. Hoi, Learning from noisy data with robust representation learning, in: *Proceedings of the IEEE/CVF International Conference on Computer Vision*, 2021, pp. 9485–9494.
- L. Jiang, D. Huang, M. Liu, W. Yang, Beyond synthetic noise: Deep learning on controlled noisy labels, in: *International conference on machine learning*, PMLR, 2020, pp. 4804–4815.
- J. Yan, L. Luo, C. Xu, C. Deng, H. Huang, Noise is also useful: Negative correlation-steered latent contrastive learning, in: *Proceedings of the IEEE/CVF Conference on Computer Vision and Pattern Recognition*, 2022, pp. 31–40.
- C. Zhang, S. Bengio, M. Hardt, B. Recht, O. Vinyals, Understanding deep learning requires rethinking generalization, in: *5th International Conference on Learning Representations, ICLR 2017, Toulon, France, April 24–26, 2017, Conference Track Proceedings*, OpenReview.net, 2017. URL: <https://openreview.net/forum?id=Sy8gdB9xx>.
- K. Sohn, D. Berthelot, N. Carlini, Z. Zhang, H. Zhang, C. A. Raffel, E. D. Cubuk, A. Kurakin, C.-L. Li, Fixmatch: Simplifying semi-supervised learning with consistency and confidence, *Advances in neural information processing systems* 33 (2020) 596–608.
- Z. Zhao, L. Zhou, L. Wang, Y. Shi, Y. Gao, Lassl: Label-guided self-training for semi-supervised learning, in: *Proceedings of the AAAI conference on artificial intelligence*, volume 36, 2022, pp. 9208–9216.
- L. Wang, R. Chan, T. Zeng, Probabilistic semi-supervised learning via sparse graph structure learning, *IEEE transactions on neural networks and learning systems* 32 (2020) 853–867.
- N. Gu, M. Fan, D. Meng, Robust semi-supervised classification for noisy labels based on self-paced learning, *IEEE Signal Processing Letters* 23 (2016) 1806–1810.
- L. Zhang, D. Xie, Y. Li, A. Camargo, D. Song, T. Lu, J. Jeudy, D. Dreizin, E. R. Melhem, Z. Wang, et al., Improving sensitivity of arterial spin labeling perfusion mri in alzheimer’s disease using transfer learning of deep learning-based asl denoising, *Journal of Magnetic Resonance Imaging* 55 (2022) 1710–1722.
- A. Krizhevsky, G. Hinton, et al., Learning multiple layers of features from tiny images (2009).
- L. Bossard, M. Guillaumin, L. Van Gool, Food-101–mining discriminative components with random forests, in: *Computer Vision–ECCV 2014: 13th European Conference, Zurich, Switzerland, September 6–12, 2014, Proceedings, Part VI* 13, Springer, 2014, pp. 446–461.
- E. Malach, S. Shalev-Shwartz, Decoupling" when to update" from" how to update", *Advances in neural information processing systems* 30 (2017).
- H. Wei, L. Feng, X. Chen, B. An, Combating noisy labels by agreement: A joint training method with co-regularization, in: *Proceedings of the IEEE/CVF conference on computer vision and pattern recognition*, 2020, pp. 13726–13735.
- H. Song, M. Kim, J.-G. Lee, Selfie: Refurbishing unclean samples for robust deep learning, in: *International Conference on Machine Learning*, PMLR, 2019, pp. 5907–5915.
- K. Yi, J. Wu, Probabilistic end-to-end noise correction for learning with noisy labels, in: *Proceedings of the IEEE/CVF conference on computer vision and pattern recognition*, 2019, pp. 7017–7025.
- X. Peng, K. Wang, Z. Zeng, Q. Li, J. Yang, Y. Qiao, Suppressing mislabeled data via grouping and self-attention, in: *Computer Vision–ECCV 2020: 16th European Conference, Glasgow, UK, August 23–28, 2020, Proceedings, Part XVI* 16, Springer, 2020, pp. 786–802.
- L. Huang, C. Zhang, H. Zhang, Self-adaptive training: beyond empirical risk minimization, *Advances in neural information processing systems* 33 (2020) 19365–19376.
- Y. Zhang, S. Zheng, P. Wu, M. Goswami, C. Chen, Learning with feature-dependent label noise: A progressive approach, arXiv preprint arXiv:2103.07756 (2021).
- J. Han, P. Luo, X. Wang, Deep self-learning from noisy labels, in: *Proceedings of the IEEE/CVF international conference on computer vision*, 2019, pp. 5138–5147.